UNDER PEER REVIEW

Direct Numerical Simulation of Mixed Convection Flow in Lid-Driven Cavities

Abstract

The mixed convection of heat transfer and fluid flow in a lid-driven cubical cavity filled with air is investigated numerically in this study. The computational procedure is based on the finite volume method and a full multigrid acceleration solver. The top wall of the cavity is maintained at a constant high-temperature T_h, and it can move with a constant velocity U_0. The bottom wall is immobile and maintained at a cold temperature T_c. While, the remaining boundary parts of the cavity are motionless and kept thermally insulated. Several numerical simulations were conducted to investigate mixed convection heat transfer in a sliding cubical cavity for a range of Reynolds numbers from 1000 to 5000 and Richardson numbers from 0.001 to 10. The influence of mixed convection parameters, Reynolds number, Richardson number, and heat transfer rate on the flow behavior was analyzed through parametric studies. The results include flow and heat transfer characteristics, iso-surfaces, and streamlines for the entire range of Richardson numbers and Reynolds numbers investigated. The study shows that as Reynolds number is increased beyond a critical value, the flow becomes unstable and bifurcates.

Keywords: Mixed convection, Richardson number, and lid-driven cavity.

Nomenclature

H	Side of cubic cavity (m)
g	Gravitational acceleration (m s^{-2})
Nu_{hot}	Average Nusselt number at the top wall
p_0	Pressure scale
P	Dimensionless pressure
Pr	Prandtl number
Re	Reynolds number
Ri	Richardson number
t	Non dimensional time
t_0	Time scale
T	Temperature
T_c	Temperature of cold wall
T_h	Temperature of hot wall
T_r	Reference temperature
u,v,w	Velocity components in x,y and z directions
U,V,W	Dimensionless velocity components
x,y,z	Cartesian coordinates
X,Y,Z	Dimensionless coordinates

Greek symbols

α	Thermal diffusivity (m^2 s^{-1})
β	Thermal expansion coefficient (K^{-1})
ν	Kinematic viscosity (m^2 s^{-1})
θ	Dimensionless temperature ((T -Tc)/ ΔT)
ρ	Density (kg m^{-3})

1. Introduction

Numerous studies [1-10] have focused on investigating mixed convection in rectangular or square cavities in the field of incompressible fluid flow research. These cavities are of interest in many industrial and engineering applications, such as cooling electronic components, lubrication technologies, food drying processes, solar power collectors, drying technologies, nuclear reactors, glass production, high-performance building insulation, and chemical processing equipment.

2. Selected bibliography

Extensive research has been conducted in the literature on the flow and heat transfer phenomena caused by buoyancy and shear forces in enclosures. One example is the numerical study of Moallemi and Jang [11] who conducted numerical simulations to study the impact of Reynolds number ($100 \leq Re \leq 2200$) and small-to-moderate Prandtl number ($0.01 \leq Pr \leq 50$) on the flow and heat transfer characteristics in a cavity for different Richardson numbers. The study revealed that the effect of buoyancy on flow and heat transfer is more significant for higher values of Pr when Re and Gr are held constant. The contribution of natural convection always enhances the magnitude of forced convection, and the overall result depends on a function of Pr and Ri. Additionally, a correlation for the average Nusselt number based on the Prandtl number, Reynolds number, and Richardson number was derived. The effects of a sliding lid on the fluid flow and thermal structures in a shallow lid-driven cavity was explored in the following study by Mohamed and Viskanta [12]. The analysis indicates that the heat transfer rate rises with increasing Reynolds number or decreasing Richardson number. Although the flow exhibits three-dimensionality and vortex formation, the local Nusselt number change along the sliding lid in the transverse direction is insignificant. The region with the maximum local heat transfer rate is located at the beginning of the sliding lid. Moreover, the impact of the return flow on the bottom of the cavity amplifies the heat transfer rate in the region of impingement. Another study was carried out by Iwatsu [13], which investigated three-dimensional flows in cubical containers with a top moving wall that is maintained at a higher temperature than the bottom wall. Numerical solutions were obtained for a wide range of physical parameters, including $Pr = 0.71$, $102 \leq Re \leq 2\times103$, and $0 \leq Ri \leq 10$, and the numerical flow visualizations showed the explicit effects of Ri as well as Re.

Meanwhile, Prasad and Koseff [14] conducted experimental research on mixed convection flow in a lid-driven cavity for a range of Richardson numbers from 0.1 to 1000. Their findings indicate that the overall heat transfer rate has very little correlation with the Grashof number in the examined range of Reynolds numbers. Additionally, they analyzed mean heat flux values over the entire boundary to create useful correlations for the Nusselt number and Stanton number in design applications. Later, Cheng and Liu [15] investigated the effect of temperature gradient orientation on mixed convection flow and heat transfer in a lid-driven square cavity. The study considers four different directions of temperature gradients and uses the Richardson number as the governing parameter. The results show that the orientation of the temperature gradient has a significant impact on the flow field and heat transfer characteristics. The assisting buoyancy flows have the best performance on heat transport, while the stable temperature gradient inhibits fluid motions and results in mainly conduction heat transfer. The unstable temperature gradient promotes natural convection, and the interaction of buoyancy and shear force results in the formation of counter-recirculating vortices. Using a numerical investigation, Aydin et al. [16] involve the transport mechanism of laminar mixed convection in a cavity that is driven by both shear and buoyancy forces,

with a locally heated lower wall and cooled moving sidewalls. Parametric studies were carried out to analyze the effect of the mixed convection parameter, Richardson number (Ri), which ranged from 0.1 to 10, on the fluid flow and heat transfer. The results showed three different regimes as the value of Ri increased: forced convection (with negligible natural convection), mixed convection (with comparable forced and natural convection), and natural convection (with negligible forced convection). Another numerical investigation is carried out by Oztop and Dagtekin [17] to study the steady-state, two-dimensional mixed convection problem in a vertically oriented, two-sided lid-driven differentially heated square cavity. The left and right walls are subjected to different constant temperatures, while the top and bottom walls are thermally insulated. Three cases are considered depending on the direction of the moving walls. The governing parameter is the Richardson number, which characterizes the heat transfer regime in mixed convection ($0.01 \leq Ri \leq 100$). The study reveals that both the Richardson number and the direction of the moving walls have a significant impact on the fluid flow and heat transfer in the cavity. In the study done by Sharif [18], the laminar mixed convective heat transfer in two-dimensional shallow rectangular driven cavities of aspect ratio 10 was numerically investigated with supplementary flow visualization. The top moving plate of the cavity was set at a higher temperature than the bottom stationary plate, and computations were reported for Rayleigh numbers ranging from 10^5 to 10^7 while maintaining a fixed Reynolds number of 408.21. This encompassed a wide spectrum of flow regimes, including dominating forced convection, mixed convection, and dominating natural convection. The fluid Prandtl number was taken as 6 to represent water. The objective of the authors was to investigate the heat transfer rate inside a lid-driven cubical cavity with an active top wall maintained at a hot temperature, while the inactive walls were insulated and the enclosure's bottom wall was cooled. The heat transfer rate was evaluated over a broad range of Reynolds numbers (Re) and Richardson numbers (Ri). The study explored both steady and unsteady behavior within a range of Reynolds numbers from Re=1000 to 5000, and identified a critical value of Reynolds number at which the flow becomes unstable and bifurcates. Numerical simulations were conducted by Abbasian et al. [19] to investigate the mixed convection flow of Cu-water nanofluid in a lid-driven square cavity with sinusoidal heating on sidewalls. The study examined the effects of varying the buoyancy force for a fixed shear force, and increasing the shear force for a fixed buoyancy force. The impacts of changes in Richardson number, phase deviation of sinusoidal heating, and volume fraction of nanoparticles on flow and temperature fields were also studied. The results showed that at all Richardson numbers, a clockwise eddy was formed inside the cavity for a constant Grashof number, and the heat transfer rate increased with decreasing Richardson number and increasing volume fraction of nanoparticles. The clockwise eddy was observed up to Ri = 1 for a constant Reynolds number. For Ri = 10, a multicellular flow pattern was observed inside the cavity. The study also found that when the Reynolds number was held constant, the rate of heat transfer increased with an increase in the Richardson number. Effect of varying inclination angle ($\varphi = 0°$-$90°$), Richardson number (Ri = 0.01, 1 and 100), and aspect ratio (A = 0.2, 1 and 5) on the mixed convective heat transfer of air within a 2-D lid-driven rectangular enclosure are investigated systematically by Cheng and Liu [20]. The flow is induced by a shear force from the motion of the cooled upper lid combined with buoyancy force due to bottom heating. The numerical findings reveal that, for a forced convection dominated regime (Ri=0.01), the flow structures and the heat transfer are not affected by an increase in inclination angle. However, for a pure natural convection-dominated regime (Ri=100, $Ra=7.1 \times 10^5$) in cavities with A=1 and 5, an increase in inclination angle increases the heat transfer rate, and the maximum heat transfer rate is achieved at $\varphi=75°$. Furthermore, under certain inclination angles, the flow transitions from a stable, laminar regime to an unstable, chaotic regime. Khorasanizade and Sousa [21] study the lid-driven cavity problem at moderate

Reynolds numbers $100 \leq Re \leq 3200$ using an ISPH method, which is a numerical technique for simulating fluid flows. A new boundary condition treatment was also tested to improve the accuracy of the simulation near solid walls. The results showed good agreement with reference data and demonstrated the potential of ISPH methods for accurately simulating fluid flows. Numerical analysis was performed by Jmai et al. [22] to investigate the laminar mixed convection in a two-sided lid-driven square cavity, filled with Cu/water nanofluid, and partially heated by two heat sources on the side walls. The top and bottom walls of the cavity are considered to be at low temperatures, and the remaining parts are thermally insulated. The top and bottom walls can slide in the same or opposite directions with various speed ratios called λ. The effects of λ ($-2 \leq \lambda \leq 2$), Richardson number Ri ($0.01 \leq Ri \leq 100$), and solid volume fraction ($0 \leq \phi \leq 0.1$) on the flow and heat transfer are studied. The results show that varying λ has significant effects on the flow structure and heat transfer. The presence of nanoparticles enhances the heat transfer and this effect is amplified by decreasing the Richardson number. A characteristic Richardson number of equilibrium, Ri_e, leading to an equal heat transfer rate balance between the two opposite sources is predicted. Additionally, multiple correlations in terms of Richardson number and volume fraction nanoparticles are established at various speed ratios. The problem of mixed convection in a square enclosure with a moving wall in an arc shape is examined numerically by Ismael [23]. The results of the study demonstrate that the direction of rotation of the lid, the radius of the arc-shaped lid, and the speed of rotation all significantly impact both the flow structure and the rate of heat transfer.

Recently, Rahman et al. [24] discuss a numerical simulation of natural convection flow in a tilted nanofluid-saturated porous cavity under the influence of a sloping magnetic field and an exothermic chemical reaction administered by Arrhenius kinetics. The study uses the Buongiorno nanofluid model and Galerkin weighted residual type of finite element method to simulate the dimensionless stream function for flow, temperature for heat, and nanoparticles volume fraction for concentration. The results show that Rayleigh and Frank-Kamenetskii numbers strongly control the convective flows, and the average Nusselt number increases with the Frank-Kamenetskii number while it decreases with the Rayleigh number. A study on mixed convection heat transfer in a cavity driven by an oscillating lid using the lattice Boltzmann method is presented by H. Lamarti et al. [25]. The study investigates the effects of Reynolds and Grashof numbers, lid oscillation frequency, and temperature on fluid flow and heat transfer characteristics. The results show that the variation of these parameters has an effect on energy transport process and drag force behavior depending on the conduct of the velocity cycle. The results also showed that the shear force on the sliding lid increases with increasing Reynolds number and lid frequency, while it decreases with increasing Grashof number.

More recently, Keya et al. [26] present a numerical investigation of mixed convection in a heat exchanger with a double pipe, where the upper lid is given a constant velocity. The study explores the effects of three governing parameters, namely Prandtl number, Richardson number, and Reynolds number, on streamlines, isotherms, and heat transfer rate. The results show that higher values of Ri and Re and lower values of Pr lead to maximum heat transfer, and the flow strength increases with time, resulting in multiple vortices. The authors of [27] present a numerical investigation of steady-state laminar mixed convection heat transfer and entropy generation in a lid-driven wavy cavity filled with aluminum oxide nanofluid. The cavity is influenced by an inner conductive solid body, and partial slip is considered at the upper moving surface. The primary focus of the analysis is to examine the effects of various parameters on flow characteristics, heat transfer control, and energy losses. Through a comprehensive examination, the study provides valuable insights into the interplay between

these parameters and their impact on the system's behavior. The results show that At Ri =0.01, the isotherms portray a nearly horizontal stratification and the natural convection is weak. Increasing Ri up to 100 results in substantial dispersion of isotherms within the cavity, leading to a reduction in the thermal boundary layer thickness at the heated partition. This, in turn, facilitates a notable increase in the local heat transfer rate on the hot undulations, thanks to the enhanced flow circulation around the solid block and the augmented buoyancy forces. Consequently, the local Nusselt number reaches its peak over the undulation crests, and a noteworthy enhancement in the average Nusselt number can be achieved when Ri is equal to or greater than 100.

3. Problem description

In this study, the three-dimensional lid-driven cubic cavity configuration depicted in Figure 1 is considered, with a Newtonian incompressible fluid (Pr = 0.71). The cavity's top lid is set to a constant high temperature T_h, while the other side walls remain adiabatic. The bottom wall is fixed and maintained at a cold temperature T_c account for three-dimensional inclination effects, the cavity is inclined around the x-axis in the present study.

To describe the mixed convection phenomenon in laminar, incompressible flow, the Boussinesq approximation can be considered, and the effects of viscous dissipation can be ignored. Under these conditions, the equations of conservation that govern the fluid dynamics can be expressed in a dimensionless form that accounts for the three-dimensional and time-dependent nature of the system as:

Continuity equation:

$$\frac{\partial u_i}{\partial x_i} = 0 \tag{1}$$

Three momentum equations:

$$\frac{\partial u_i}{\partial t} + \frac{\partial (u_i u_i)}{\partial x_j} = -\frac{\partial P}{\partial x_i} + \frac{1}{\mathrm{Re}}\left(\frac{\partial^2 u_i u_i}{\partial x_i \partial x_i}\right) + Ri\theta\delta_{i3} \tag{2}$$

Energy equation:

$$\frac{\partial \theta}{\partial t} + \frac{\partial (u_i \theta)}{\partial x_i} = \frac{1}{\mathrm{Re}\,\mathrm{Pr}}\left(\frac{\partial^2 \theta}{\partial x_i \partial x_i}\right) \tag{3}$$

Where, *u*, *v* and *w* are the velocity components in the *x, y* and *z* directions, respectively, θ is the temperature and P is the pressure. ρ is the mass density and g is the gravitational acceleration. In Eq. (2), the symbol δ stands for the Krönecker delta. The chosen scales in Eqs. (1)– (3) are:

the length H ,

the reference velocity $u_0 = \sqrt{g\beta H \Delta T}$,

the time $t_0 = \frac{H}{u_0}$

and the pressure $P_0 = \rho u_0^2$

Further, the dimensionless temperature is defined by $\theta = (T - T_r)(T_h - T_c)$, where the reference temperature is $T_r = \frac{(T_h + T_c)}{2}$.

Correspondingly, the dimensionless numbers that emerge are the Grashof number, Gr, Reynolds number, Re, Prandtl number, Pr, and and Richardson number Ri, which are defined as:

$Gr = \frac{g\beta\Delta T L^3}{\nu^2}$, $\mathrm{Re} = \frac{u_0 L}{\nu}$, $\mathrm{Pr} = \frac{\nu}{\alpha}$ and $Ri = \frac{Gr}{\mathrm{Re}^2}$, respectively.

The boundary conditions for the problem include no-slip conditions at the bottom and side walls of the cavity, while the upper lid has a prescribed constant velocity u_0 and a hot temperature T_h.

4. Numerical approach and validation

4.1. Numerical method

A FORTRAN home code was used to implement a numerical method and solve the governing equations numerically. The non-linear terms in Eqs. (2) were treated explicitly using a second-order Adams–Bashforth scheme, while the convective terms in Eq. (3) were treated semi-implicitly. The diffusion terms in Eqs. (2) and (3) were treated implicitly. To overcome the challenge of the strong velocity-pressure coupling, we adopted a projection method as described in Brown and Cortez [28]. The Navier-Stokes-Boussinesq and energy equations are discretized using a finite-volume method (Patankar [29], Moukhalled [30], Kobayashi [31]). To minimize numerical diffusion for the advective terms in Eqs. (2), the QUICK scheme of Hayase et al. [32] is employed. The Poisson pressure correction equation is solved using a full multi-grid method [33]. The red and black points successive over-relaxation method [34] is used to solve the discretized equations with optimized relaxation factors. Solutions converge when the relative error for each dependent variable between two consecutive iterations falls below the convergence criterion ε, which is recorded, such that:

$$\sum_{i,j,k} \left| \phi_{ijk}^{m+1} - \phi_{ijk}^{m} \right| \le \varepsilon$$

Here, ϕ represents a dependent variable u, v, w, or θ. The superscript m indicates the iteration number and the subscript sequence (i, j, k) represents the space coordinates x, y and z. The convergence criterion was set to 10^{-6}.

4.2. Code validation

The 3D lid-driven cubic cavity test case was simulated using our in-house three-dimensional finite volume code and validated against the works of Wong et al. [1]. Table 1 presents the comparison results for the average Nusselt number. We have chosen a grid of 64^3 nodes refined near the walls. Fig. 2 displays a comparison of u- and W-velocity profiles along the centerline of the heated lid-driven cubical cavity of the current study with Ref. [11, 35] at Reynolds numbers Re = 1000. The results show good agreement between the various

solutions. Our data, along with the centerline profiles, is in good agreement with the results of Ref. [1]. The average Nusselt number computed was also compared and validated, further enhancing confidence in the numerical outcome of the present work.

5. Results and discussion

Fig. 1 displays the configuration of the computational model used to simulate the 3D lid-driven cubic cavity flows.
The lid of the cubic cavity maintains a constant temperature Th and moves parallel to the positive x-axis at a steady velocity U = U0 = 1, while the bottom wall is kept at a temperature $T_c<T_h$. The remaining walls are thermally insulated. It is to note that a uniform Cartesian mesh with a resolution of 64^3 nodes is employed to simulate these flows.

The flow inside the cubic cavity is influenced by both the Reynolds and Richardson numbers. In order to investigate the behavior of the lid-driven cubic cavity, simulations are conducted for a range of Reynolds numbers from 1000 to 5000, and for various Richardson numbers. The simulations encompass both the steady field at Reynolds number of 1000, and the fully developed unsteady laminar field at Reynolds number of 2000.

Plots of the U –velocity and the W –velocity components along the vertical centerlines on the symmetry plane are shown in Fig.3 The U-velocity profile exhibits the same trend for all Reynolds numbers at each Richardson number. For Ri= 0.001, the U –velocity profile indicates the presence of a clockwise rotating cell covering most of the cavity domain. At Ri= 1 and Ri= 10, the U-velocity components are nearly zero in the lower part of the cavity due to the thermal stability of the flow in that zone. In the upper half of the cavity, a clockwise rotating cell emerges.

Concerning the plots of the W-velocity components, they exhibit the same trend for all Reynolds numbers at Ri = 0.001 and Ri = 1. When the Richardson number is small, the W-velocity components are positive in the left half of the cavity and negative in the right half, indicating a clockwise rotating flow. When Ri = 1, a cell appears near the right half of the cavity. For Ri = 10, the W-velocity is minimal, suggesting thermal stratification throughout the cavity for all Reynolds numbers.

By considering the Reynolds hypothesis, one can decompose the instantaneous velocity into its mean value and a fluctuating component. Consequently, this can be expressed as:
$\overline{u_i} = \langle \overline{u_i} \rangle + \overline{u'}_i$, where $\overline{u'}_i$ is the fluctuating part.
The turbulence intensities are defined by the following dimensionless expressions:

$$U_{rms} = 10\sqrt{\left\langle \left(\overline{u'}\right)^2 \right\rangle} \quad \text{and} \quad W_{rms} = 10\sqrt{\left\langle \left(\overline{w'}\right)^2 \right\rangle}$$

Fig. 4 displays the profiles of U_{rms} and W_{rms}. As observed, as the Reynolds number increases, the velocity fluctuations become more significant in the predominance of forced convection (Ri=0.001), and the flow becomes more unsteady. In contrast, for Ri=1, large

fluctuations are shown in U_{rms} and W_{rms} profiles, irrespective of Re. When natural convection predominates (Ri = 10), U_{rms} fluctuations are practically null in half bottom of the cavity. It is also noted that the increase of the Reynolds number does not affect much the U-velocity fluctuations near the lid-driven plate. However, by increasing Re, the W_{rms} profiles are clearly different. Indeed, the corresponding fluctuations are especially important as the Reynolds number increases.

The iso-surfaces for various velocity magnitudes for Reynolds numbers (Re) ranging from 1000 to 5000 and for different values of Richardson number (Ri) varying from 0.001 to 10 are presented in Fig.5. Iso-surfaces are three-dimensional surfaces that represent particular values of the velocity magnitude in a fluid. In this case, iso-surfaces are used to represent the magnitude of fluid velocity in turbulent flow. The graph is presented as a grid of several subplots, each subplot representing a specific combination of Reynolds and Richardson values. Reynolds values are represented on the horizontal axis of each subplot, while Richardson values are represented on the vertical axis. Examining the graph, one can see that the iso-surfaces are very complex and vary considerably depending on the Reynolds and Richardson values.

In the cases of Ri =10, the iso-surfaces represent a thermally stratified state, indicating that the buoyancy forces are the major driving forces controlling the fluid flow behavior. In such a state, the heat transfer is primarily governed by conduction, suggesting that the contribution of forced convection due to the lid's motion is negligible. This is because the buoyancy forces caused by the temperature differences are much stronger than the forces caused by the motion of the lid. This suggests that the fluid flow is stable and laminar in nature, with a relatively constant velocity distribution.

For Ri=1, the behavior of the iso-surfaces changes, indicating that the flows become unsteady but still remain laminar, we can see that the iso-surfaces came closer to each other, some perturbations are visible in the center of the cavity. However, a thermally stratified state still exists and the buoyancy effects continue to dominate.

At low Richardson numbers, such as Ri=0.001, and for Re=1000 the behavior of the iso-surfaces changes considerably, indicating that the flows become unsteady. The iso-surfaces become more complex and irregular, with areas of high and low velocity mixing together. This suggests that the fluid flow behavior becomes unstable as the Richardson number is decreased, and a transition to unsteady and turbulent flow is presented. These effects are accentuated by increasing the Reynolds number.

Overall, the interpretation of this figure is that the stability and behavior of the fluid flow is strongly influenced by the values of the Reynolds and Richardson numbers. The Reynolds number represents the ratio of inertial forces to viscous forces in the fluid flow, while the Richardson number represents the ratio of buoyancy forces to viscous forces. By varying these parameters, it is possible to observe different types of fluid flow behavior, ranging from stable and laminar to unsteady and turbulent.

Fig. 6 displays the distribution of mid-plane streamlines for various combinations of Re and Ri values. At Re=1000 and Ri=10, the flow pattern exhibits five main counter-rotating vortices, which are mainly influenced by the fluid motion near the hot sliding wall. As the Ri decreases to unity, the flow is characterized by two large clockwise and anticlockwise vortices, along with a smaller secondary recirculating vortex induced by buoyancy near the bottom wall. On the other hand, for Ri=0.001, a single primary vortex dominates the cavity domain.

At Re=5000 and Ri=10, a primary vortex appears on the right side of the hot wall due to the movement of the lid, and minor cells are observed in the remaining part of the cavity. For Ri=1, this primary cell shifts towards the center of the cube, and the minor vortices disappear. A similar trend is observed for Ri=0.001 at Re=1000.

The 2D plane projections of the velocity vector field, at Re=1000 and for different Richardson number investigated, on the three centroidal planes of the cube are presented in Fig.7, offering insights into the flow behavior. At x=0.5 plane, two eddies are observed in the upper half region that gradually move towards the cube center and bottom corners as the Richardson number decreases.

In the case of the y=0.5 plane, it is found that a single vortex occupies the region near the hot sliding wall. This behavior is mainly due to the lid movement. As the Richardson number decreases, the volume of this vortex expands inside the cavity. At Ri=0.001, a single primary vortex is observed, which covers most of the cavity domain. The trend indicates that the vortex structure is more predominant at lower Richardson numbers.

Looking at the z=0.5 plane, at Ri=10, the flow is found to be stagnant in the center of the cavity, indicating stable and laminar flow. However, as the Richardson number decreases to Ri = 1, a pair of vortices appears near the centerline and moves out towards the left corners. Further reduction of the Richardson number to 0.001 leads to a significant increase in the vortex strength and size, indicating the transition to the turbulent regime. Therefore, the Richardson number is a critical parameter in determining the flow behavior inside the cavity.

Alternatively, Fig.8 presents the 2D plane projections of the velocity vector field at Reynolds number 5000, showcasing various Richardson numbers. The visualization reveals a dynamic and fluctuating behavior in both planes x=0.5 and z=0.5. The presence of unsteadiness can be observed from the oscillations in the velocity vectors, indicating that the flow is unstable and continuously evolving over time. The fluctuations are more apparent as the Richardson number decreases, which highlights the importance of this parameter in dictating the flow behavior. Focusing on the y=0.5 plane, it was observed that the behavior was similar to that of Re=1000. Overall, these results suggest that the unsteady behavior observed in the velocity vector field is highly dependent on the Reynolds number and Richardson number of the flow, and can be attributed to the complex interplay between buoyancy effects and flow dynamics.

Figure 9 illustrates the Iso-surface of the vertical velocity component W at the y=0.5 center plane, depicting various Reynolds and Richardson numbers. The graph is presented as a grid of several subplots, each subplot representing a specific combination of Reynolds and

Richardson values. Reynolds values are represented on the horizontal axis of each subplot, while Richardson values are represented on the vertical axis. The iso-surfaces are colored using a color scale ranging from dark red to light blue to indicate high and low velocity areas. Red areas indicate ascendant velocity or positive velocity, while blue areas indicate descendant velocity or negative velocity zones. By looking at the figure, you can likely observe how the behavior of the flow changes as the Reynolds number and the Richardson number vary. For example, at low Reynolds numbers, the flow may be more laminar and regular, while at high Reynolds numbers, it may become more turbulent and chaotic. Similarly, at high Richardson numbers, the flow may be more stratified, while at low Richardson numbers, it may become more homogeneous and well-mixed.

6. Conclusion

In this study, numerical results for mixed convection heat transfer in a sliding cubical cavity has been analyzed. The computations were performed using the finite volume method, and a full multigrid acceleration was applied to solve the incompressible viscous fluid problems.

The geometry of the cavity consisted of a hot isothermal top wall that was moving, a cold bottom wall that was at rest, and thermally insulated sidewalls. The study investigated several Reynolds numbers ranging from 1000 to 5000, covering both steady and unsteady flow regimes.

The results of the study were obtained for different ranges of important parameters, such as Reynolds numbers and Richardson numbers. For each Reynolds number, the Richardson number was varied from 0.001 to 10.

In test case, it’s found that the results of the computations agreed well with other numerical solutions.

The study revealed that at Reynolds numbers varying from Re=1000 to 5000, intrinsic 3D properties such as corner eddies were observed for different Richardson numbers. Velocity profiles along the vertical centerline in the symmetry plane are presented at Re=1000 and 5000. The results indicate that the stability and behavior of the fluid flow are strongly influenced by the values of the Reynolds and Richardson numbers, which showed both steady and unsteady behavior. Overall, the interpretation of the figures suggests that the fluid flow behavior becomes unstable as the Richardson number is decreased, and a transition to unsteady and turbulent flow is presented.

The findings of the study provide valuable insights into the nature of mixed convection heat transfer in a sliding cubical cavity and can be used to inform the design of related engineering systems.

7. References

[1]K.L. Wong, A.J. Baker, A 3D incompressible Navier–Stokes velocity–vorticity weak form finite element algorithm, Int. J. Numer. Meth. Fluids 38 (2002) 99-123. *https://doi.org/10.1002/fld.204*

[2]A.K. Hussein and S. H. Hussain, Mixed convection through a lid-driven air-filled square cavity with a hot wavy wall, Int. J. Mech. Mater. Eng 5 (2010) 222-235. *https://www.researchgate.net/publication/289168743*

[3]H. Nemati, M. Farhadi, K. Sedighi, E. Fattahi, A. A. R. Darzi, Lattice Boltzmann simulation of nanofluid in lid-driven cavity. Int. Commun. Heat Mass Transf. 37 (2010) 1528-1534. *https://doi.org/10.1016/j.icheatmasstransfer.2010.08.004*

[4]G.A. Sheikhzadeh, M. Ebrahim Qomi, N. Hajialigol, A. Fattahi, Numerical study of mixed convection flows in a lid-driven enclosure filled with nanofluid using variable properties, Results Phys. 2 (2012) 5-13. *https://doi.org/10.1016/j.rinp.2012.01.001*

[5]H. Hassanzadeh Afrouzi and M. Farhadi, Mix Convection Heat Transfer in a Lid Driven Enclosure Filled by Nanofluid, Iran. J. Energy Environ. 4 (2013) 376-384. *DOI: 10.5829/idosi.ijee.2013.04.04.09*

[6]Arash Karimipour, Mohammad Hemmat Esfe, Mohammad Reza Safaei, Davood Toghraie Semiromi, Saeed Jafari, S.N. Kazi, Mixed convection of Copper-Water nanofluid in a shallow inclined lid driven cavity using lattice Boltzmann method, Physica A 402 (2014) 150-168. *https://doi.org/10.1016/j.physa.2014.01.057*

[7]Rehena Nasrin, M.A. Alim, Ali J. Chamkha, Modeling of mixed convective heat transfer utilizing nanofluid in a double lid driven chamber with internal heat generation, Int. J. Numer. Methods Heat Fluid Flow 24 (2014) 36-57. *http://dx.doi.org/10.1108/HFF-11-2011-0239*

[8]Abdelkader Boutra, Karim Raguia and Youb Khaled Benkahla, Numerical study of mixed convection heat transfer in a lid driven cavity filled with a nanofluid, Mech. Ind. 16 (2015). *https://doi.org/10.1051/meca/2015027*

[9]N. A. Bakar, A. Karimipour and R. Roslan, Effect of Magnetic Field on Mixed Convection Heat Transfer in a Lid-Driven Square Cavity, J. Thermodyn. 1 (2016) 1-14. *https://doi.org/10.1155/2016/3487182*

[10] Mohammad Mastiani, Myeongsub Mike Kim, Ali Nematollah, Density maximum effects on mixed convection in a square lid-driven enclosure filled with Cu-water nanofluids Adv. Powder Technol. 28 (2017) 197–214. *https://doi.org/10.1016/j.apt.2016.09.009*

[11] Moallemi, M. K. and Jang, K. S. Prandtl number effects on laminar mixed convection heat transfer in a lid-driven cavity. Int. J. Heat Mass Transf. 35 (1992) 1881-1892. https://doi.org/10.1016/0017-9310(92)90191-T

[12] A.A.Mohamed, R.Viskanta, Flow and heat transfer in a lid-driven cavity filled with a stably stratified fluid, Appl. Math. Model. 19 (1995) 465-472. https://doi.org/10.1016/0307-904X(95)00030-N

[13] R. Iwatsu and J.M. Hyun, Three-dimensional driven-cavity flows with a vertical temperature gradient, Int. J. Heat Mass Transf. 38 (1995) 3319–3328. https://doi.org/10.1016/0017-9310(95)00080-S

[14] Prasad, A. K. and Koseff, J. R. Combined forced and natural convection heat transfer in a deep lid-driven cavity flow. Int. J. Heat Fluid Flow 17 (1996) 460-467. https://doi.org/10.1016/0142-727X(96)00054-9

[15] T.S. Cheng, W.-H. Liu, Effect of temperature gradient orientation on the characteristics of mixed convection flow in a lid-driven square cavity, Comput. Fluids 39 (2010) 965-978.

[16] O. Aydin, W.-J. Yang, Mixed convection in cavities with a locally heated lower wall and moving sidewalls, Numer. Heat Transfer A Appl. 37 (2000) 695-710. https://doi.org/10.1080/104077800274037

[16] H.F. Oztop, I. Dagtekin, Mixed convection in two-sided lid-driven differentially heated square cavity, Int. J. Heat Mass Transfer 47 (2004) 1761-1769. https://doi.org/10.1016/j.ijheatmasstransfer.2003.10.016

[17] M. A. R. Sharif, Laminar mixed convection in shallow inclined driven cavities with hot moving lid on top and cooled from bottom, Appl. Therm. Eng. 27 (2007) 1036-1042. https://doi.org/10.1016/j.applthermaleng.2006.07.035

[18] A.A. Abbasian Arani, S. Mazrouei Sebdani, M. Mahmoodi, A. Ardeshiri, M. Aliakbari, Numerical study of mixed convection flow in a lid-driven cavity with sinusoidal heating on sidewalls using nanofluid, Superlattices Microstruct. 51 (2012) 893-911. https://doi.org/10.1016/j.spmi.2012.02.015

[19] T.S. Cheng, W.-H. Liu, Effects of cavity inclination on mixed convection heat transfer in lid-driven cavity flows, Comput. Fluids 100 (2014) 108-122. http://dx.doi.org/10.1016/j.compfluid.2014.05.004

[20] S. Khorasanizade, J.M. Sousa, A detailed study of lid-driven cavity flow at moderate Reynolds numbers using Incompressible SPH, Int. J. Numer. Meth. Fluids 76 (2014) 653-668. https://doi.org/10.1002/fld.3949

[21] R. Jmai, B. Ben-Beya, T. Lili, Numerical analysis of mixed convection at various walls speed ratios in two-sided lid-driven cavity partially heated and filled with nanofluid, J. Mol. Liq. 221 (2016) 691-713. http://dx.doi.org/10.1016/j.molliq.2016.05.076

[22] M. A. Ismael, Numerical solution of mixed convection in a lid-driven cavity with arc-shaped moving wall, Eng. Comput., 34 (2017) 869-891. http://dx.doi.org/10.1108/EC-11-2015-0368

[23] M.M. Rahman, I. Pop, M.Z. Saghir, Steady free convection flow within a titled nanofluid saturated porous cavity in the presence of a sloping magnetic field energized by an

exothermic chemical reaction administered by Arrhenius kinetics, Int. J. Heat Mass Transf., 129 (2019) 198-211.
https://doi.org/10.1016/j.ijheatmasstransfer.2018.09.105

[24] H. Lamarti, M. Mahdaoui, R. Bennacer, A. Chahboun, Numerical simulation of mixed convection heat transfer of fluid in acavity driven by an oscillating lid using lattice Boltzmann method, Int. J. Heat Mass Transf.,137 (2019) 615-629.
https://doi.org/10.1016/j.ijheatmasstransfer.2019.03.057

[25] S.T. Keya, S. Yeasmin, M.M. Rahman, M.F. Karim, M.R. Amin, Mixed convection heat transfer in a lid-driven enclosure with a double-pipe heat exchanger, Int. J. of Thermofluids, 13 (2022) 100-131.
https://doi.org/10.1016/j.ijft.2021.100131

[26] Ammar I. Alsabery, Mohammad H. Yazdi, Ali S. Abosinnee, Ishak Hashim, Evgeny Solomin, Impact of partial slip condition on mixed convection of nanofluid within lid-driven wavy cavity and solid inner body, Propul. Power Res. 11 (2022) 544-564.
https://doi.org/10.1016/j.jppr.2022.09.001

[27] D.L. Brown, R. Cortez, M.L. Minion, Accurate projection methods for the incompressible Navier–Stokes equations, J. Comput. Phys. 168 (2001) 464-499.
https://doi.org/10.1006/jcph.2001.6715

[28] S.V. Patankar, A calculation procedure for two-dimensional elliptic situations, Numer. Heat Transfer 34 (1981) 409-425.
https://doi.org/10.1080/01495728108961801

[29] F. Moukhalled and M. Darwish, A unified formulation of the segregated class of algorithm for fluid flow at all speeds, Numer. Heat Transfer B Fundam. 37 (2000) 103-139.
https://doi.org/10.1080/104077900275576

[30] M.H. Kobayachi, J.M.C. Pereira and J.C.F. Pereira, A conservative finite-volume second-order-accurate projection method on hybrid unstructured grids, J. Comput. Phys. 150 (1999) 40-75.
https://doi.org/10.1006/jcph.1998.6163

[31] T. Hayase, J.A.C. Humphrey and R. Greif, A consistently formulated QUICK scheme for fast and stable convergence using finite-volume iterative calculation procedures, J. Comput. Phys. 98 (1992) 108-118.
https://doi.org/10.1016/0021-9991(92)90177-Z

[32] N. Ben-Cheikh, B. Ben-Beya, and T. Lili, Benchmark solution for time-dependent natural convection flows with an accelerated full-multigrid method, Numer. Heat Transfer B Fundam. 52 (2007) 131-151.
https://doi.org/10.1080/10407790701347647

[33] R. Barrett, M. Berry, T.F. Chan, et al, Templates for the Solution of Linear Systems: Building Blocks for Iterative Methods, SIAM (1994).
DOI:10.1137/1.9781611971538

[34] N. Ouertatani, N. Ben-Cheikh, B. Ben-Beya, and T. Lili, Mixed convection in a double lid-driven cubic cavity, Int. J. Thermal Sci., 48 (2009) 1265-1272.
https://doi.org/10.1016/j.ijthermalsci.2008.11.020

Table 1: Comparison of the computed average Nusselt number at the top wall for Re=1000.

Ri=0.001			Ri=1			Ri=10		
Ref[11]	Ref[23]	Pres.work	Ref[11]	Ref[23]	Pres.work	Ref[11]	Ref[23]	Pres.work
7.03	7.284	7.295	1.80	1.856	1.863	1.37	1.143	1.143

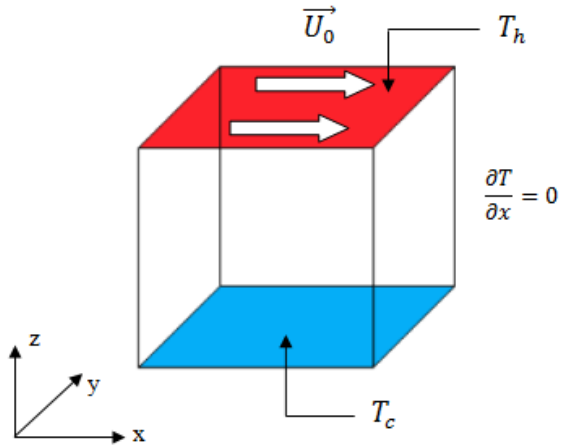

Fig. 1. Schematic diagram of the problem domain and coordinate system.

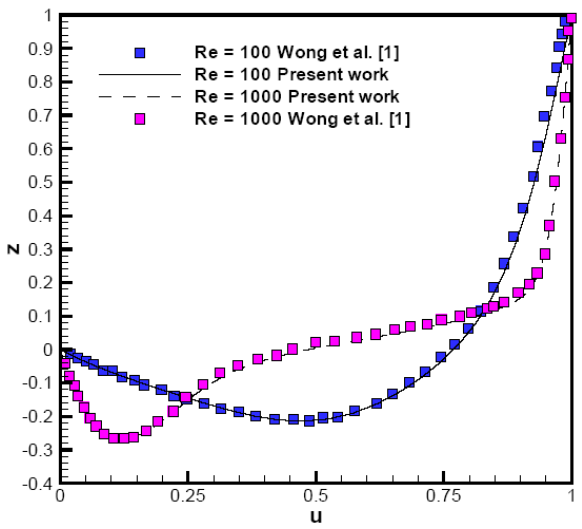

Fig. 2. Comparison of U -and W -velocity components distribution along the centerline of cubic cavity of the present work with Ref. [1] for Re = 100 and 1000.

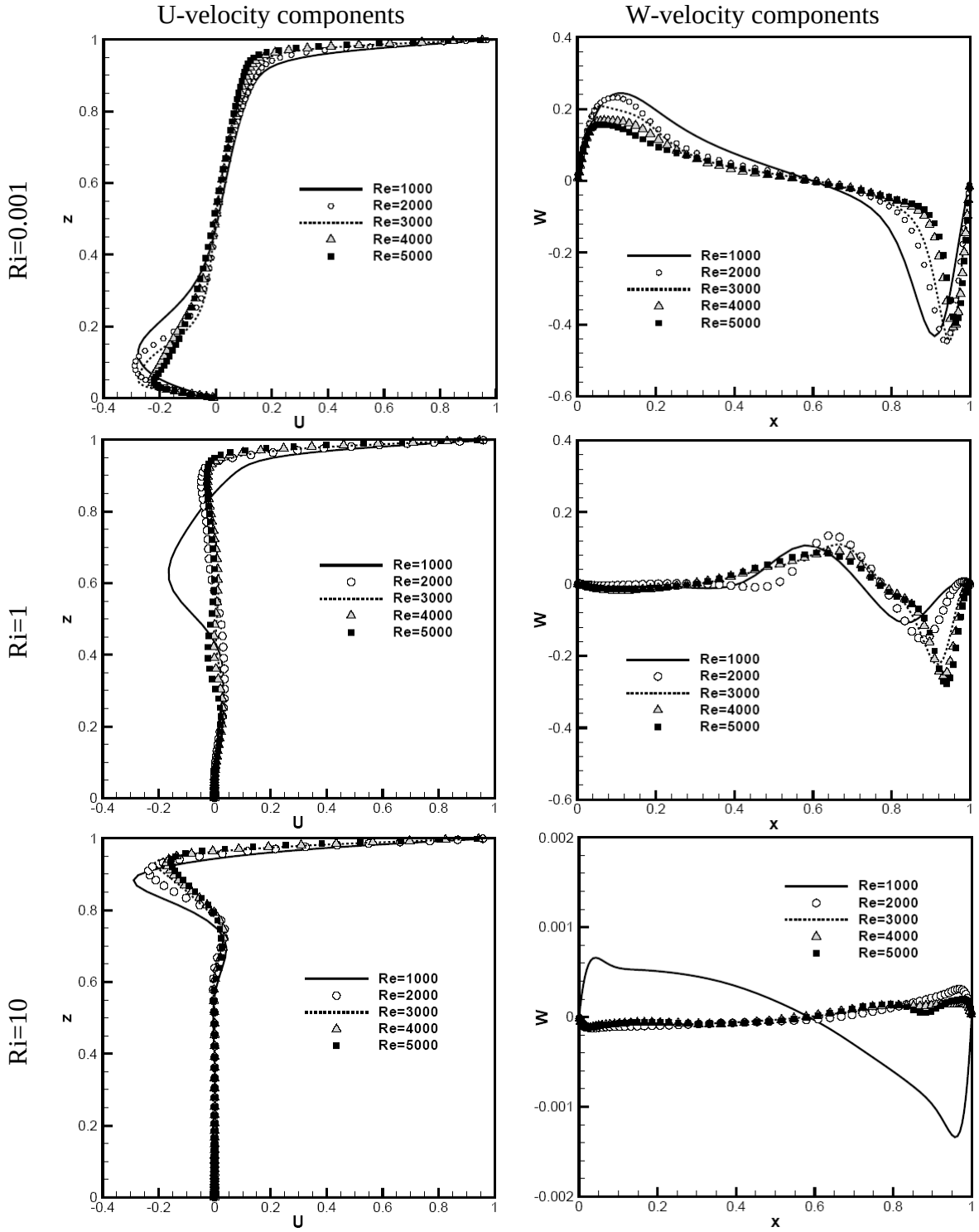

Fig.3. U-velocity and W-velocity components at the centerline y = 0.5 for different Reynolds numbers at different Richardson numbers.

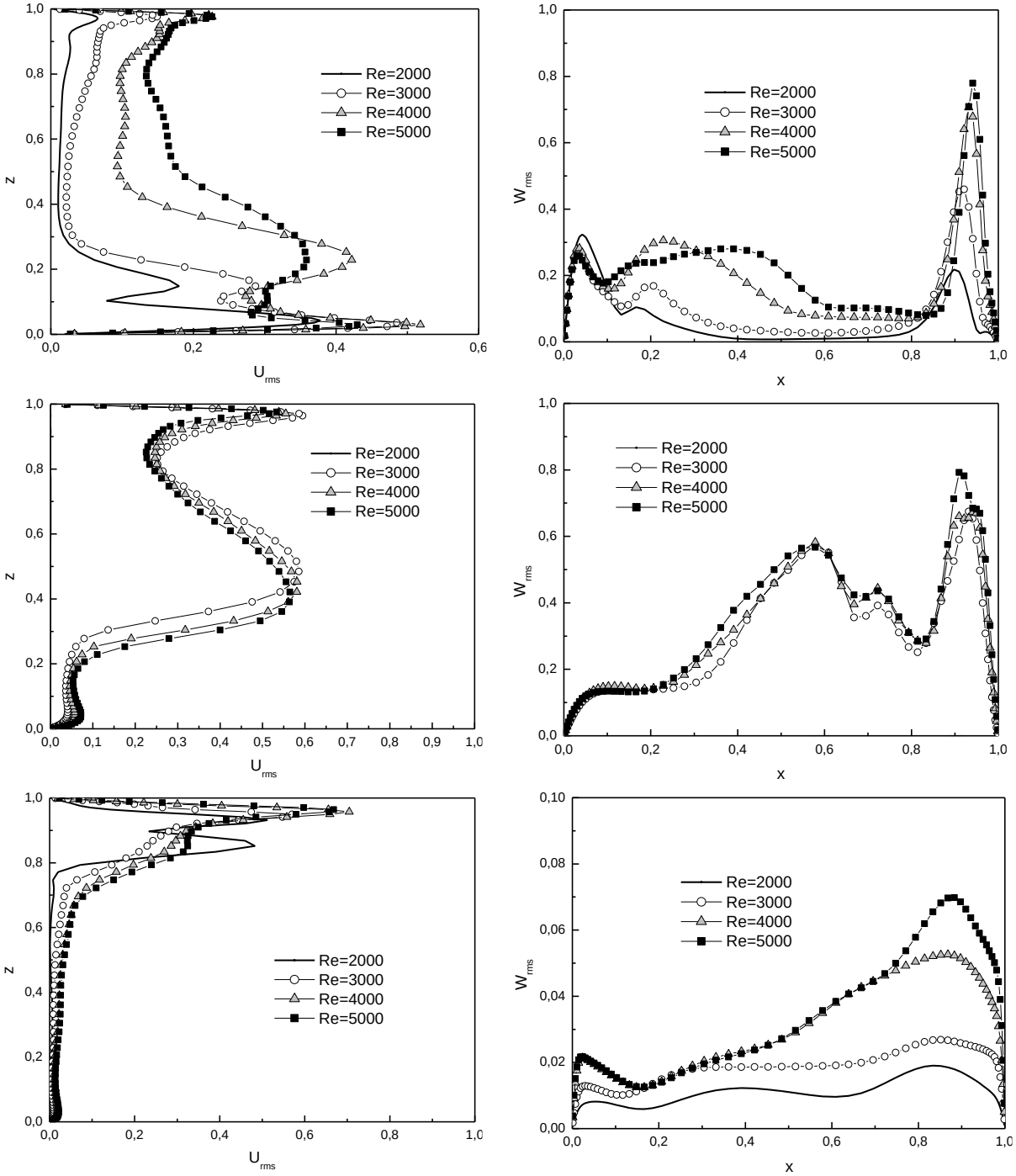

Fig.4. The U_{rms} and W_{rms} profils for different Reynolds numbers at Ri =0.001(top), 1 (middle) and 10 (bottom).

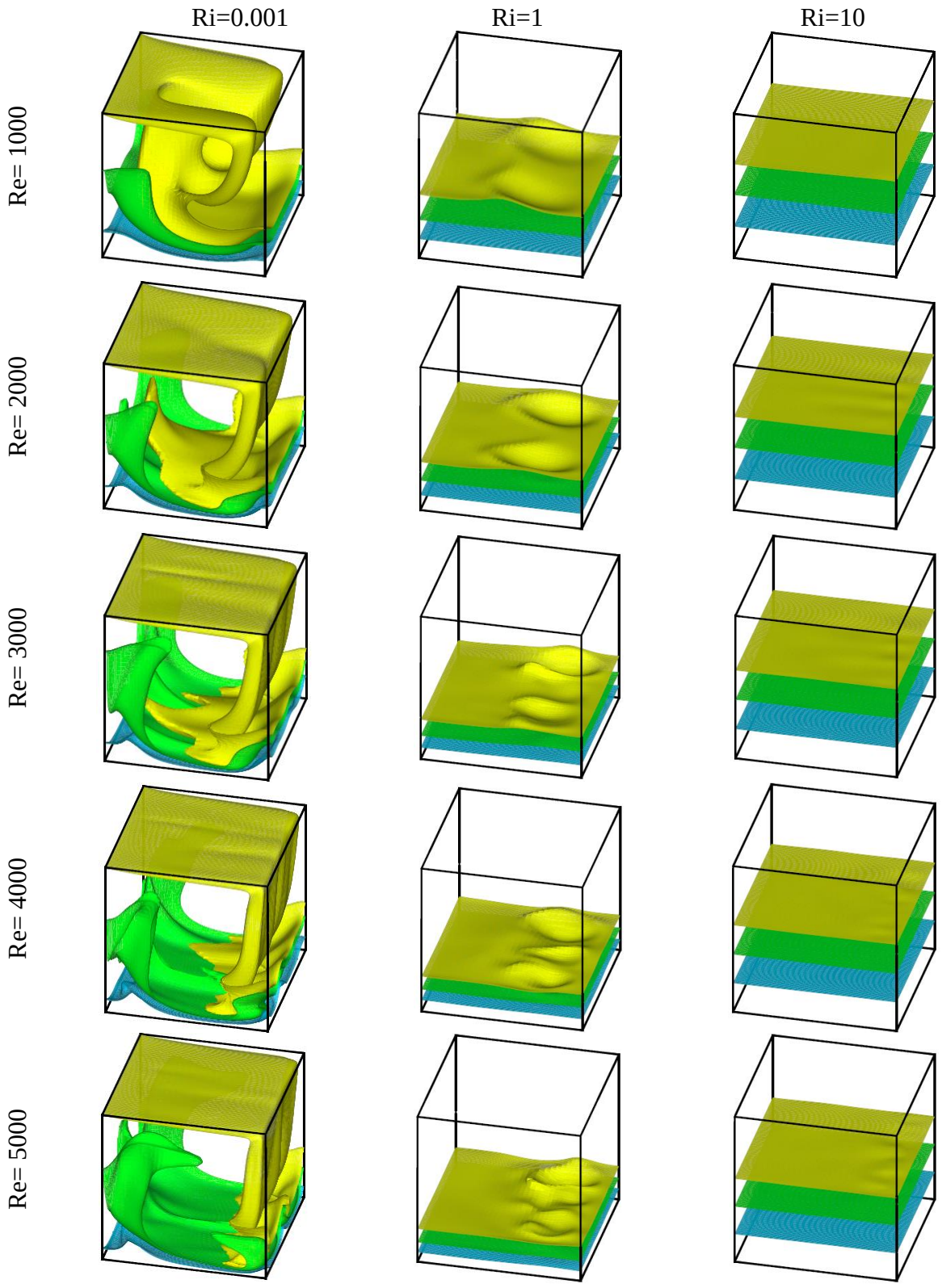

Fig. 5. Iso-surfaces of velocity magnitudes for different Reynolds and Richardson numbers

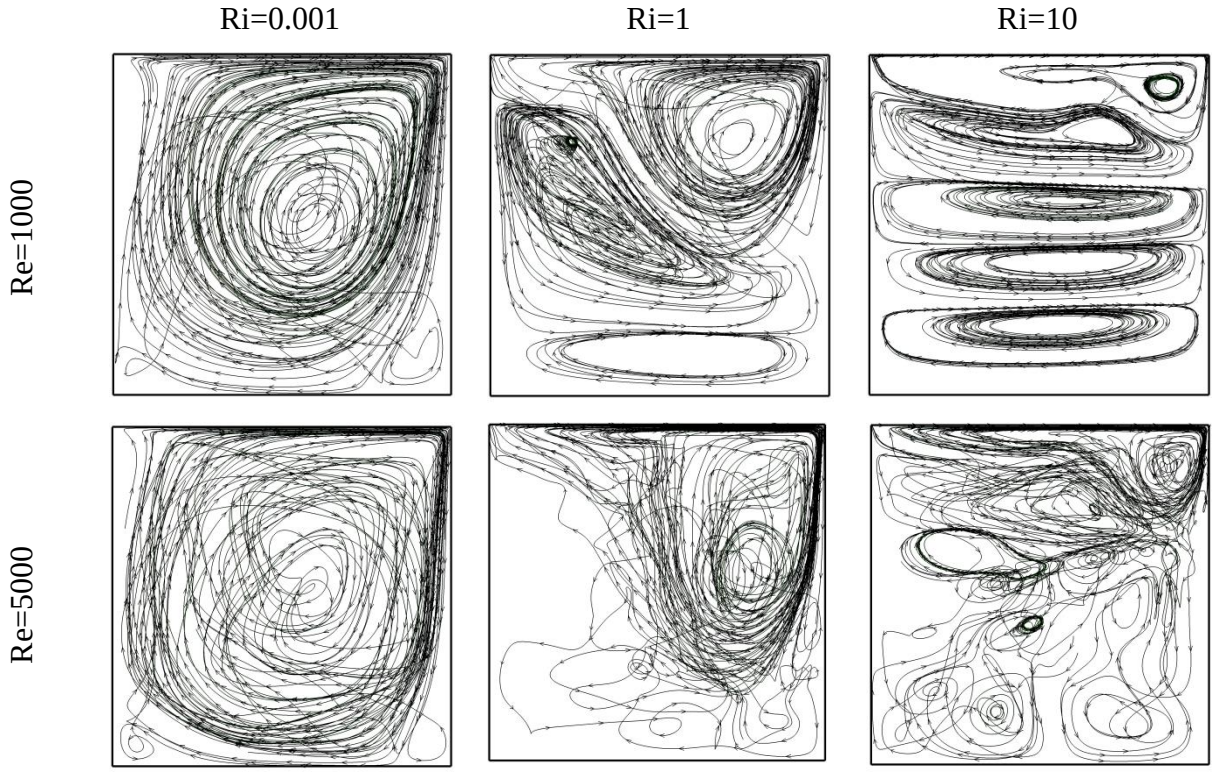

Fig. 6. Streamtraces at the mid-plane (y = 0.5) at Re = 1000 and Re = 5000 for the three Richardson numbers Ri = 0.001, 1 and 10.

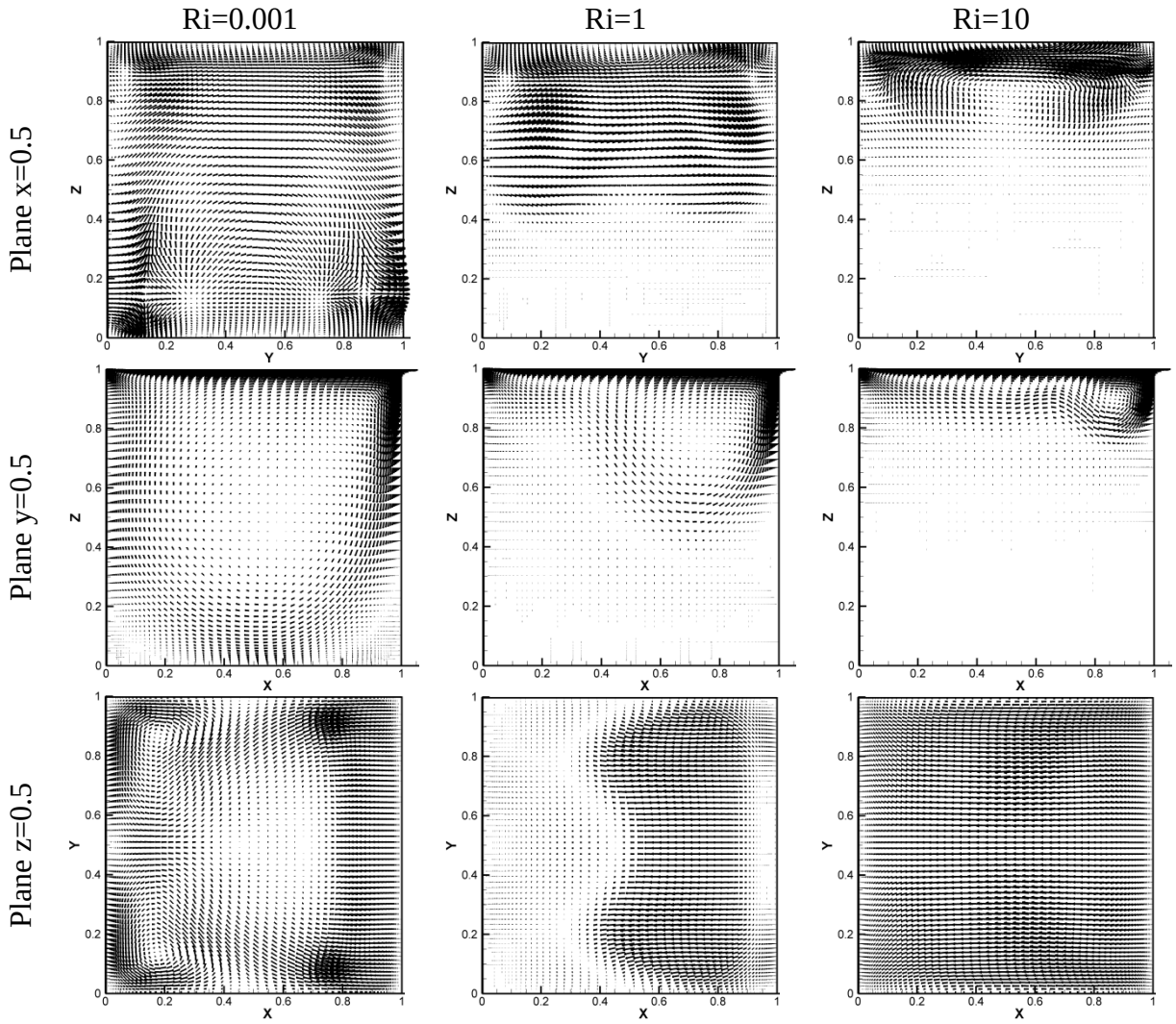

Fig. 7. Projections of mid-plane velocity vector for different Richardson number at Re=1000 on different planes: x=0.5 ; y=0.5 and z=0.5.

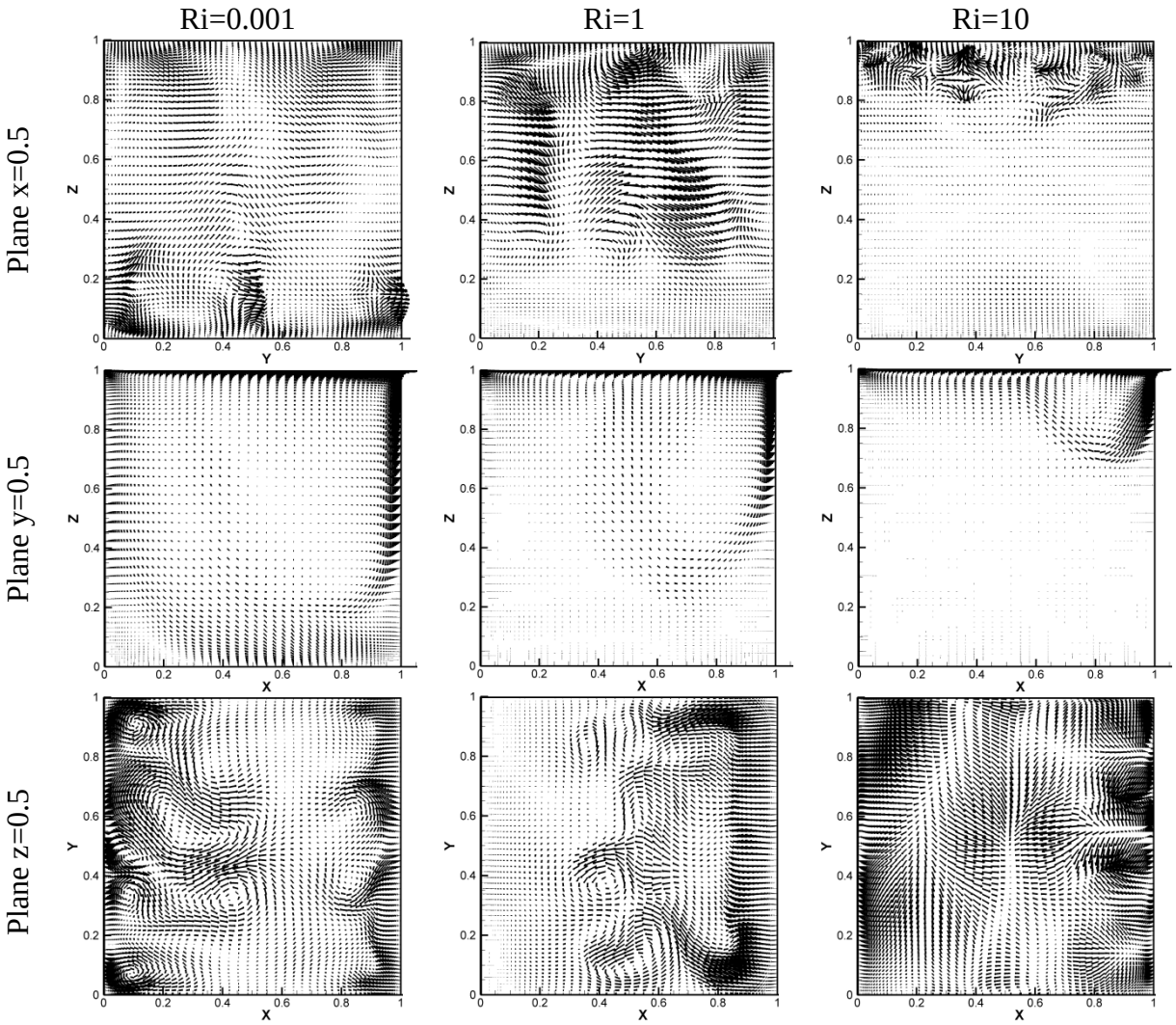

Fig. 8. Projections of mid-plane velocity vector for different Richardson number at Re=5000 on different planes: x=0.5 ; y=0.5 and z=0.5.

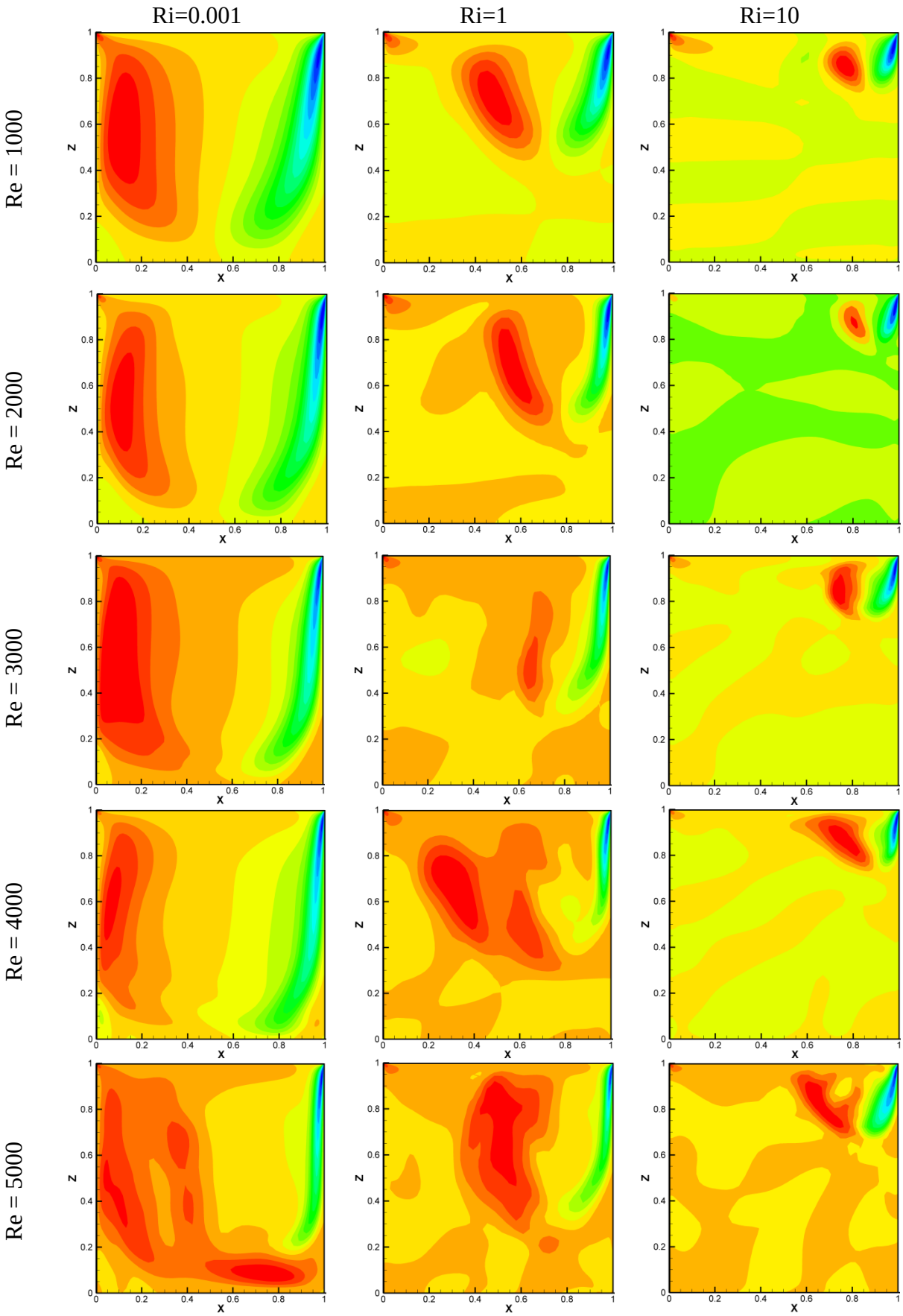

Fig. 9. Iso-surface of the vertical velocity component W at y=0.5 for different Reynolds numbers and different Richardson numbers.